CHAPTER - 4

EXPERIMENTAL MEASUREMENTS

In this chapter the method, experimental arrangement and other details of measurement will be described separately for each of the three experiments which were set up and carried out in course of the present investigation. The results obtained from the measurements will also be presented with proper mention of the errors involved and corrections employed.

4.1 γ-ray transmission experiment :

A narrow beam of γ-rays is weakened when it is made to traverse a material specimen. The incident beam decreases in intensity because the sample absorbs and scatters it. The loss of intensity of the traversing beam is called attenuation. A measure of the amount of attenuation is the "attenuation coefficient". At low energies, the removal of photons from the incident beam is caused mainly by photo-electric absorption, coherent (elastic) scattering and incoherent (Compton) scattering. The cross sections for these partial processes can be estimated to adequately high accuracies using various degrees of sophistication in theoretical models. Experimentally, the total photon-atom interaction cross sections are determined by conducting a narrow beam transmission experiment on a good geometry set up.

A. Method:

The conventional derivation of the photon attenuation applies to cases with both narrow beam geometry and monoenergetic photons. The result is summarised in the Beer-Lambert Law

$$I = I_o \, e^{-\mu_m x}$$

connecting the incident beam intensity I_o, the transmitted intensity I and the thickness X (gm/cm^2) of the target fixed perpendicular to the beam. μ_m is the mass attenuation coefficient defined by

$$\mu_m = \sigma \left(\frac{N}{A} \right)$$

Where A is the atomic weight of the atom in the target sample, N is the Avogadro's number (6.022×10^{23}) and σ is the photon-atom interaction cross section. We obtain

$$\sigma = \left(\frac{A}{N} \right) \left(- \frac{\ln I/I_o}{x} \right) \text{ barns/atom}$$

Although extensive cross section measurements by this method have been carried out and compiled[46-47] at the National Bureau of Standards (NBS) in USA, the method is still attractive and useful from the point of view of the high precision which is dependent mainly on the phton counting statistics and the geometry.

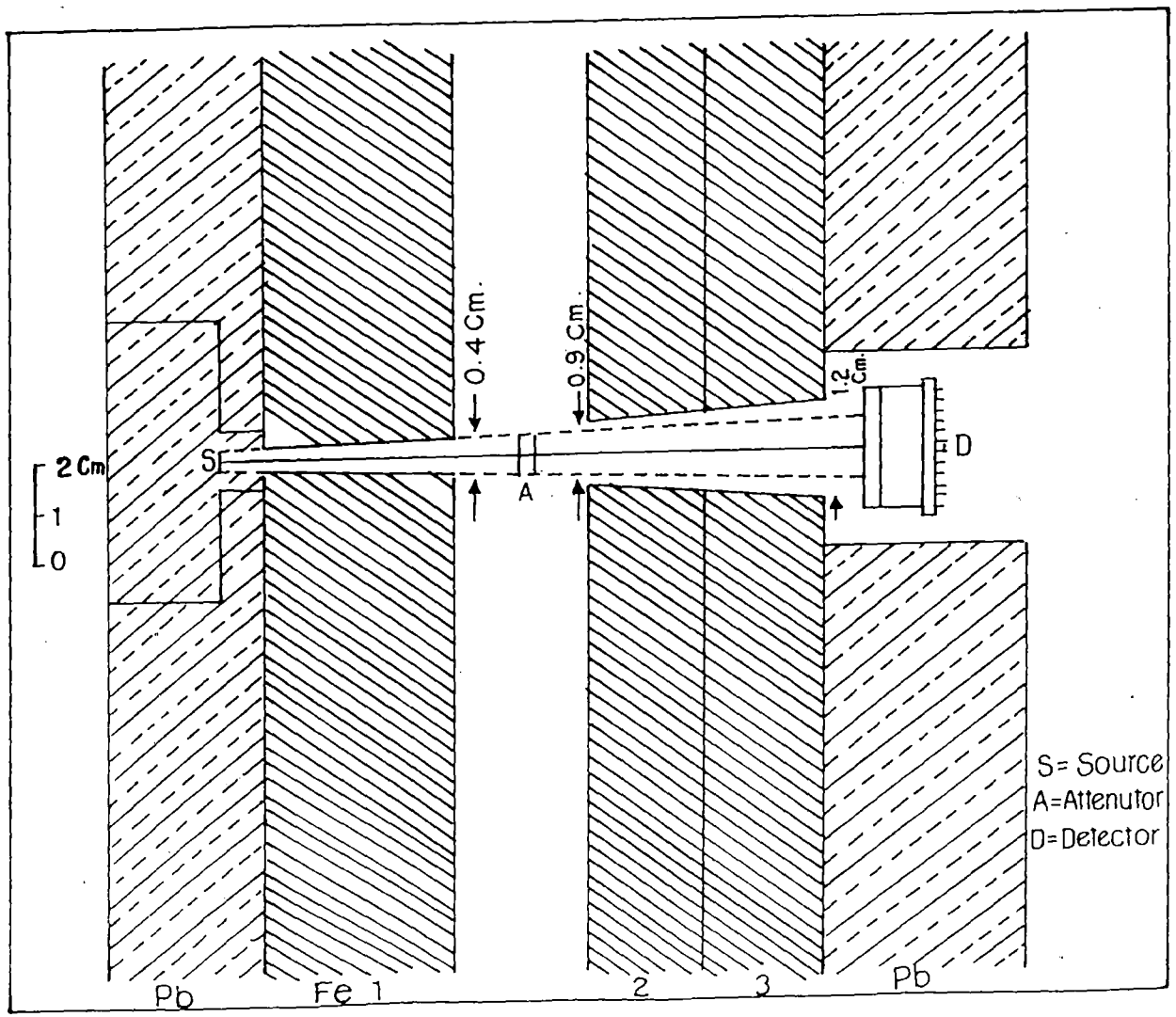
0.4 Cm.
0.9 Cm.
1.2 Cm.
2 Cm
1
0
S
A
D
Pb
Fe
1
2
3
Pb
S= Source
A=Attenutor
D=Detector

Fig 12

B. Experimental Arrangement :

The measurements were made with the transmission technique using a NaI detector in the "good geometry". The experimental arrangement employed is shown in Fig. 12. An improvement was achieved by effecting a high degree of collimation of the photon beam from the source to the detector. The source was placed in a 10 cm deep conical bore in a lead block. The minimum thickness of the lead shielding at the side and at the back of the source was 20 cm. Collimator number 1 was a 23 cm thick iron block having a collimating bore of exit aperture of 0.4 cm. The collimation of the beam after attenuation in the target foil was provided by collimators numbered 2 and 3 which had a total thickness of 15 cm of iron. The collimators prevented photons scattered in the air and the shield materials from reaching the detector. The collimators were mounted on a rigid bench of iron and could be moved so that measurements at two or more narrow beam geometries could be carried out after changes in collimator apertures. In measurements carried out with the sample 20 cm from the source, the solid angle of the collimating system between the attenuator and the detector was 3.8×10^{-4} Sr. In this geometry, the maximum angle of scattering from the attenuator to the detector was 0.3°. The detector, R 2.5 cm NaI (TI) scintillator, was shielded by 20 cm of lead and was coupled to a conventional system of photomultiplier pre-amplifier and a Nuclear Data 1100 multichannel analyser (MCA).

C. Materials and Measurement:

The photon-atom interaction cross section measurements were made on a pyrolytic graphite specimen (Z = 6) and a single crystal silicon specimen (Z = 14) for the photon energy 59.54 KeV and on thin elemental sample foils of rare-earths in the atomic number range Z = 41-70 and Z = 73, 79 and 92 using photon energies 43 and 59.54 keV. The photon beams of the specified energies were obtained from the ^{241}Am isotope of strength 20 mCi procured from Radio Chemical Centre, Amersham, England. Most of the target foils were supplied by Good Fellow Metals, Cambridge, England within a purity range 99.9 - 99.99%. Single crystal silicon specimen was obtained from International Union of Crystallography X-ray attenuation project.

For each absorber the ratio (I_o/I) was obtained in the obvious way from the counting rates

N = Counting rate with absorber in position

N_o = Counting rate with empty sample holder

N_b = background rate with γ-rays off.

$$\frac{I_o}{I} = \frac{N_o - N_b}{N - N_b}$$

Counting were recorded for 2×10^3 seconds. Under study conditions of the detector system, no drift of the photo peak was detected

over at least 24 hours. The background counts were observed with the source absent and also with the source and attenuator in position in conjunction with a 20 cm long stopper placed in the beam behind the attenuator and collimators 2 and 3. The difference between these two count rates of the background was negligibly small. In most of the cases, measurements were repeated at the same solid angle between the attenuator and the detector for each sample and the mean value of (I_o/I) was taken. For some samples, measurements were repeated by varying the solid angle of the collimating system to stuey and eliminate, by extrapolation, the effects of geometry of the experimental arrangement on the contribution of small angle photon scattering.

D. Experimental results

In table 18 the calculated experimental total interaction cross sections are presented. From the measured photon attenuation cross sections, the cross sections for photo ionisation were deduced by subtracting the theoretically estimated contributions of elastic (coherent) and inelastic (incoherent) scattering processes. Such theoretical estimates were done using the tables of Schaupp et al and Hubbell et al. The derived photoionization cross sections are presented in Table 19.

Table 18. Total photon attenuation cross sections in barns per atom

Element/Cross Section (Z) (b/atom)	E = 43 keV	E = 59.54 keV
^{6}C	-	3.4051(0.004)
^{14}Si	-	14.8430(0.004)
^{41}Nb	1548.38(39.01)	733.40(14.96)
^{42}Mo	-	686.81(1.43)
^{48}Cd	-	1242.13(3.92)
^{49}In	2767.97(53.36)	1351.78(21.72)
^{64}Gd	-	3460.92(3.92)
^{66}Dy	1495.86(7.35)	-
^{68}Er	-	4031.59(3.89)
^{70}Yb	2093.78(0.29)	941.20(3.45)
^{73}Ta	2621.96(39.95)	1060.50(15.02)
^{79}Au	3479.81(142.87)	1463.98(55.25)
^{92}U	-	2534.46(1.98)

Table 19. Measured photo-electric cross sections in barns/atom

Element/(Z)	Photo electric Cross Section (b/atom) σ_{PE}	E = 43 keV	E = 59.54 keV
	^{41}Nb	1482.30(39.02)	686.75(14.99)
	^{42}Mo	-	638.02(1.74)
	^{48}Cd	-	1179.06(4.09)
	^{49}In	2672.75(53.38)	1286.13(21.76)
	^{64}Gd	-	3348.52(4.24)
	^{66}Dy	1314.53(7.82)	-
	^{68}Er	-	3903.16(4.26)
	^{70}Yb	1885.03(2.31)	804.17(3.90)
	^{73}Ta	2391.59(40.03)	910.22(15.14)
	^{79}Au	3202.59(142.90)	1284.80(55.29)
	^{92}U	-	2282.96(3.45)

The errors quoted for the experimental results are mainly due to the counting statistics. The effect of small-angle scattering of the phton on the measured attenuation coefficient was not observed in the geometry employed. Error due to multiply scattered photons from the attenuator was minimized by very narrow collimation of the transmitted beam and by measuring transmission for very thin sample foils.

4.2 Small angle Scattering experiment.

The purpose of a scattering experiment is to measure the differential scattering cross section $\frac{d\sigma}{d\Omega}$ as a function of the angle of scattering. The total flux of photons into a detector are measured, and the differential cross section deduced. A collimated beam of photons of the chosen energy from a source is allowed to impinge on a target which scatters the beam in various directions. A shielded detector, located outside the direct beam, records the photons scattered at a pre-determined angle Θ . The detector accepts photons which emerge from the scatterer within a solid angle $d\Omega$ around direction θ .

A. Experimental arrangement:

At small angles of scattering, it is difficult to keep the detector away from the incident photon beam. The usual practice

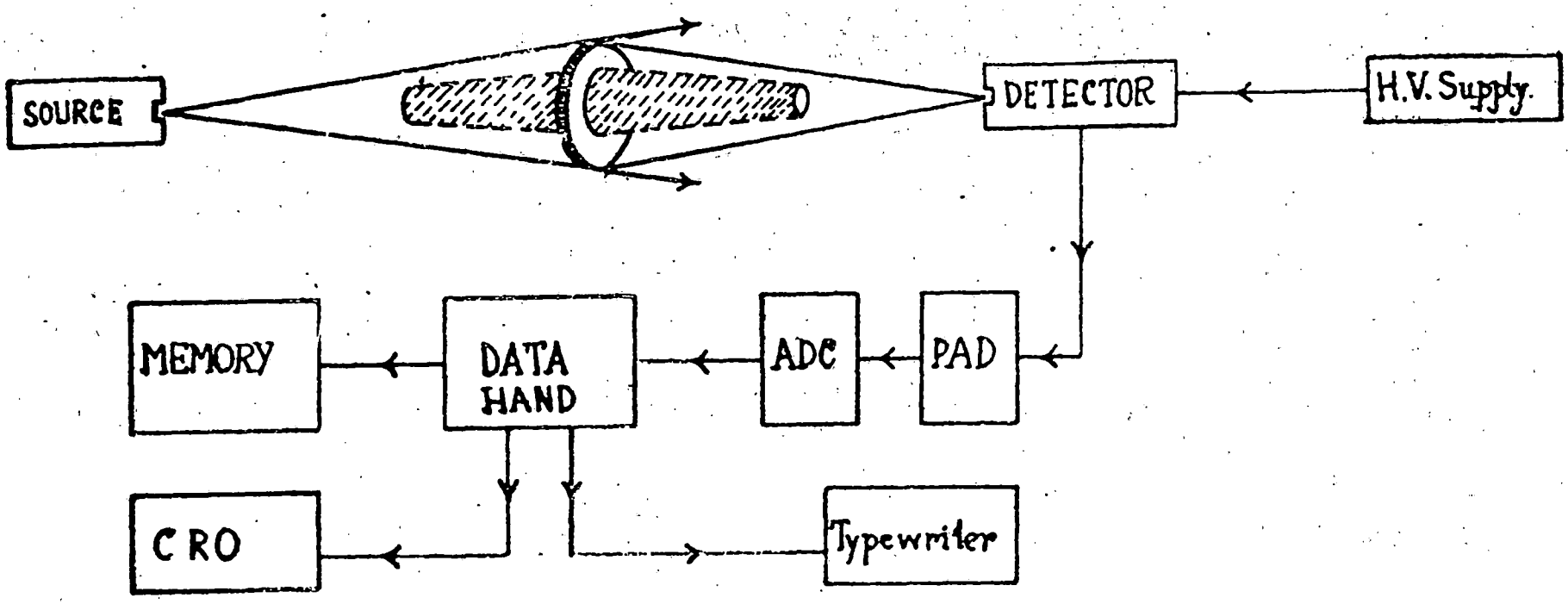
SOURCE
DETECTOR
H.V. Supply
MEMORY
DATA HAND
ADC
PAD
CRO
Typewriter

Fig 13.

is to employ a double shadow cone geometry. The experimental arrangement used in our small angle measurements is shown in Fig. 13. A double conical cylinder made of brass was suspended between the source and the detector. The straight part of the primary γ-ray beam was effectively absorbed by this shadow cone, leaving the detector completely within the shadow of the stopper. The stopper (double cone) was suspended from rigid wooden supports about 100 cm from the ground with the help of two silk strings fixed to the ends of adjustable screws.

The source, a ^{241}Am radio isotope of strength 10 mCi was placed at the rear end of a lead cylinder which had a cylindrical hole throughout its symmetry axis. The small angle scattering measurements were conducted by allowing 59.54 keV γ-rays from the source to undergo scattering from annular ring targets mounted on the double cone stopper, suspended midway between the source and the detector. A compact geometry was obtained by optimising the source to detector distance and the angle of scattering was varied by changing this distance.

The alignment of the source, the double cone stopper and the detector was carried out with great care by optical means. The fractional solid angle from the source/detector to the annular ring scatterer was limited to the range 2.2×10^{-3} - 8.5×10^{-3} for a scattering angle range of 5° - 20°. In the

geometry shown the scatterer and between the scatterer and the detector were both in the range 1 - 1.6 m.

B. Method:

The total number of photons, N_s scattered at an angle θ per unit time, both by elastic and inelastic processes in the scatterer, and recorded by the detector of efficiency ϵ, is given by

$$N_S = \frac{N_o}{4\pi r^2} \epsilon N_{at} \frac{d\sigma(\theta)}{d\Omega} \Omega_1 \exp\left(-\mu t/\cos\phi\right)$$

where N_o is the number of photons emitted by the source per unit time, r is the mean source-to-scatterer distance, N_{at} is the total number of atoms in the effective volume of the scatterer, and Ω_1 is the solid angle subtended by the detector at the scatterer. The term $\exp\left(-\mu t/\cos\phi\right)$ accounts for the absorption of photons in the target material where μ is the attenuation coefficient, t the thickness of the target and ϕ is the mean angle between the lines joining the source to the scatterer and to the detector. The determination of the detector efficiency was avoided in the present measurements through elimination of the product $\epsilon\Omega_1$ in the expression for N_s by a short comparison run with a weaker reference source of the same photon energy. How this comes about can be explained as follows.

With the source shut off, the target removed and the reference source placed in the target position, the number of counts counts registered by the detector is

$$N_{ref} = \frac{R_o}{4\pi} \epsilon \Omega_1$$

where R_o is the photon-emission rate of the reference source. It follows that

$$\epsilon \Omega_1 = \frac{4\pi}{R_o} N_{ref}$$

Using this, the expression for N_s becomes

$$N_s = \frac{N_o}{4\pi r^2} N_{at} \frac{d\sigma(\theta)}{d\Omega} \exp\left(-\mu t/\cos\phi\right) \left(\frac{4\pi}{R_o} N_{ref}\right)$$

$$= N_{ref} \left(\frac{N_o}{R_o}\right) \frac{N_{at}}{r^2} \frac{d\sigma(\theta)}{d\Omega} \exp\left(-\mu t/\cos\phi\right)$$

The absolute value of cross section $\frac{d\sigma(\theta)}{d\Omega}$ is then obtained as

$$\frac{d\sigma(\theta)}{d\Omega} = \left(\frac{N_s}{N_{ref}}\right)\left(\frac{R_o}{N_o}\right)\left(\frac{r^2}{N_{at}}\right) \exp\left(\mu t/\cos\phi\right)$$

$$= \left(\frac{N_s}{N_{ref}}\right) \frac{1}{S} \left(\frac{r^2}{N_{at}}\right) \exp\left(\mu t/\cos\phi\right)$$

The relative source strength $S = \frac{N_o}{R_o}$ was determined by taking the ratio of the photo peak count rates obtained with the strong (experimental) and the weak reference source placed at equal distances from the detector. To obtain (N_s/N_{ref}) in our measurements we first determined the rate at which scattered γ-rays from the main source were detected in the full energy peak of the pulse height spectrum. The main source was then shut off and the target was replaced by the reference source. The rate at which photons from this source was detected in the full energy peak was determined. The ratio of the two rates gave (N_s/N_{ref}).

C. Measurements:

The small angle differential measurements were made using an ND 1100 multichannel analyser system coupled to a 2.5 cm x 2.5 cm NaI (TI) scintillation detector head at a conversion gain of 1024 with 512 channels and spectrum storage times in the range $4\text{-}100 \times 10^3$ sec. The scattering materials (Cu, Sn, Ag, Ta, Au and Pb) were very pure and in the form of thin foils (thicknesses in the range 0.01-0.10 mm). The scattering counts were taken for a minimum of 10 KS. At the source-sample-detector distances used, the observed intensities were large enough to obtain desired statistical accuracy of 1%. For example, at a scattering angle of 17.7° for the lead scatterer, the total count recorded was 7.00×10^6. The background counts recorded with no target runs for the same time and experimental condition were subtracted from the total counts obtained as the sum of channel contents under the

photo peak to obtain the scattered counts.

D. Experimental results

The measured differential cross sections for total scattering (elastic + inelastic) at small angles (5° - 20°) are presented in Tables 20. The photons scattered at such small scattering angles could not be spectrally analysed to separate the inelastic component. The experimental results for Cu, Ag, Sn, Ta, Au and Pb cover a momentum transfer range of 0.018-0.037 mc. The theoretical cross section values for the elastic (Rayleigh) scattering were obtained from the numerical partial wave calculations of Kissel et al. The inelastic cross sections were calculated using the incoherent scattering factors S(q,z) from the compilation of Hubbell et al in the formula

$$\frac{d\sigma^{inel}}{d\Omega} = \frac{d\sigma^{K-N}}{d\Omega} S(q,z)$$

where $\frac{d\sigma^{K-N}}{d\Omega}$ is the differential Klien-Nishina cross section.

The corrections applied to experimental cross section data included (i) sample dependent background and (ii) the finite angular width at each scattering angle in the range 0.5° - 2°. The former needed a correction of upto 5%. The sample dependent background absorbed in the sample was obtained from $^{49}\sim B_s (1 - \mu t)$. B_s was measured from the same measurements at two scatterer

Table 20. Measured differential cross section for total (elastic + inelastic) scattering and the extracted elastic scattering cross-sections

Element (Z)	Scattering angle Θ (deg)	Momentum transfer q (mc)	Differential cross section $d\sigma/d\Omega$ (b/atom/Sr)	
			Measured	Extracted
^{29}Cu	8.9	0.018	31.88 ± 3.30	31.09
	12.6	0.023	16.89 ± 1.69	15.86
	14.2	0.029	12.99 ± 1.33	11.86
	17.7	0.036	8.26 ± 0.98	6.98
^{47}Ag	8.9	0.018	71.19 ± 7.41	70.09
	12.6	0.023	41.69 ± 4.40	40.24
	14.2	0.029	37.08 ± 4.01	35.50
	17.7	0.036	25.84 ± 2.71	24.10
^{50}Sn	8.9	0.018	88.68 ± 8.98	87.52
	12.6	0.023	52.49 ± 5.39	50.99
	14.2	0.029	41.25 ± 4.26	39.61
	17.7	0.036	31.44 ± 3.31	29.57
^{73}Ta	8.9	0.018	297.25 ± 30.43	295.85
	12.6	0.023	174.18 ± 18.41	172.34
	14.2	0.029	124.37 ± 13.23	122.37
	17.7	0.036	77.01 ± 8.31	74.74

Element (Z)	Scattering angle Θ (deg)	Momentum transfer q (mc)	Differential cross section $d\sigma/d\Omega$ (b/atom/Sr)	
			Measured	Extracted
^{79}Au	5.7	0.012	336.17 ± 34.55	335.27
	9.4	0.019	221.12 ± 23.02	219.64
	13.2	0.027	137.31 ± 14.61	135.55
	15.00	0.030	118.37 ± 12.54	116.19
	18.6	0.038	84.83 ± 9.34	82.34
^{82}Pb	8.9	0.018	238.46 ± 24.82	236.99
	12.6	0.023	162.41 ± 17.15	160.46
	14.2	0.029	151.45 ± 16.38	149.29
	17.7	0.036	109.36 ± 12.05	106.65

thicknesses, and the scattering counts were corrected accordingly. The correction for the angular spread was obtained by determining the form of variation of the theoretical differential cross section with respect to the angle in the range 1^{o} - 20^{o}; the correction was found to be within 3% for an angular spread of $\frac{\Delta\theta}{\theta} = \frac{1}{4}$.

Possible systematic and random errors have been taken into consideration in the evaluation of the measured cross sections. These include uncertainties in (i) the determination of the photo peak area of the scattered spectrum (ii) the attenuation coefficients for 59.54 keV photons in the scatterer materials; (iii) the value of the relative source strength S; and (iv) the counting and measuring sample size and distances. Systematic errors have been either exluded effectively or accounted for with appropriate corrections. The activity of the main and the reference source had an uncertainty less than $\pm$ 5% , and the attenuation coefficients for 59.5 keV photons were known to an accuracy of $\backsim$ 1%.

4.4. Large angle scattering experiment

For the large angle differential measurements the NaI detector was replaced by a high resolution intrinsic germanium detector and a configuration with plane scatterer was employed. The elastic and inelastic peaks could be separated in the pulse height spectrum and the elastic scattering cross sections differential in angle were obtained directly.

A. Experimental arrangement

The experimental arrangement used for measuring differential cross section of elastic (coherent) scattering at the angles 60° - 165° is shown in the Fig. 14. The geometry of the set up utilised a configuration with a plane scatterer positioned on the Thales circle described between the source and the detector. The angle of scattering was varied by rotating the detector about a vertical axis passing through the centre of the scatterer.

A high degree of collimation of the primary photon beam was achieved by using adequate shielding of the source. A conical bore was made through the axis of a lead cylinder and an elaborate shielding on all sides of this cylinder was made with the help of lead bricks. The ^{241}Am source sealed in a cylindrical capsule was placed in the lead housing obtained as above, the conical bore in the housing having a length of 30 cm and a diameter of 2 cm. Variou source to scatterer distances were used but in each case source-to-scatterer distance (r_1) and the scatterer-to-detector distance (were kept equal. Simultaneously, the scattering (θ) and the angle (ψ) between the direction of incident beam and the scatterer were always adjusted so as to satisfy the relation

$$\frac{r_1}{r_2} = \frac{\sin \psi}{\sin (\theta - \psi)}$$

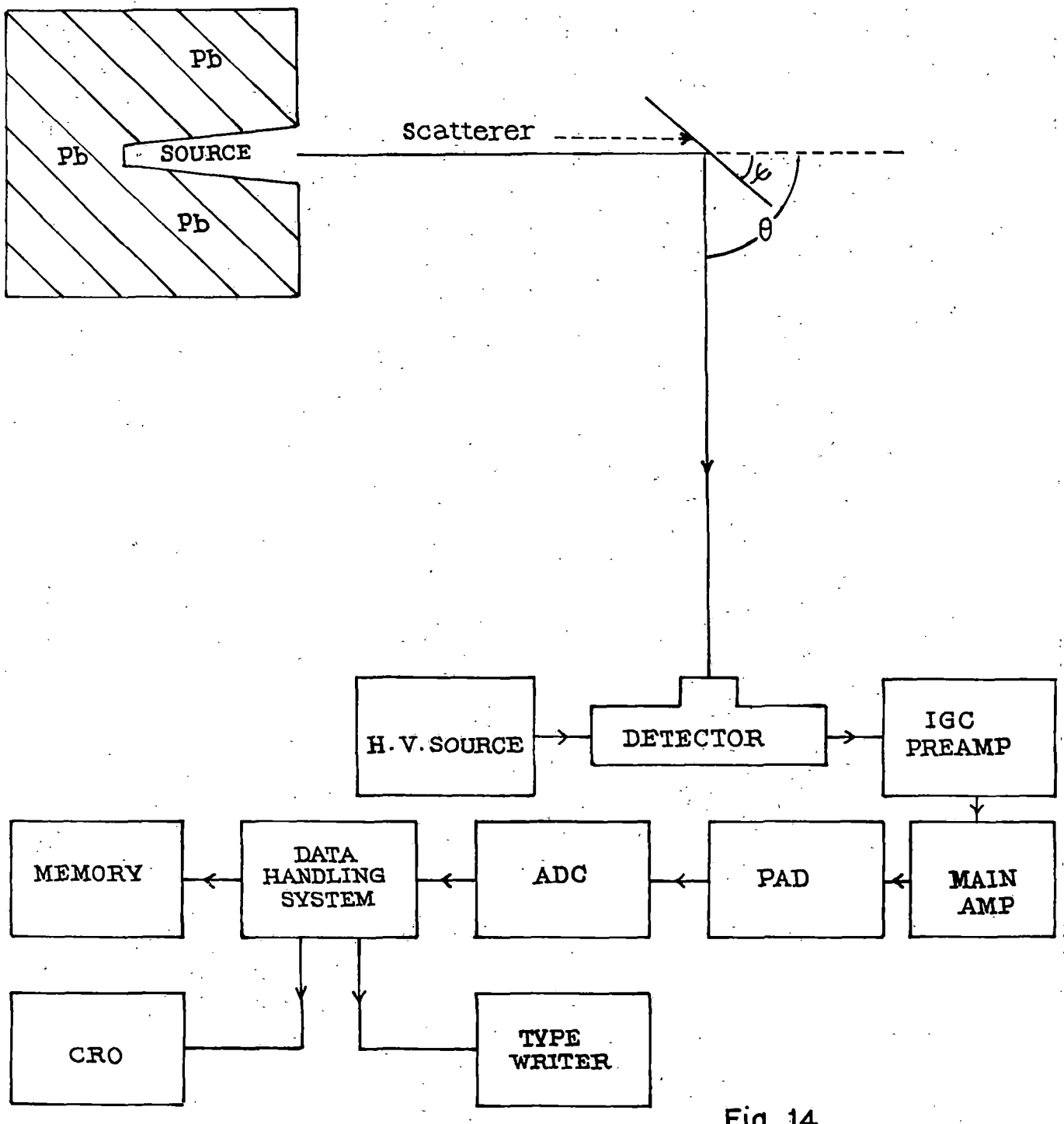
Pb
Pb
SOURCE
Pb
Scatterer
φ
θ
H.V.SOURCE
DETECTOR
IGC PREAMP
MEMORY
DATA HANDLING SYSTEM
ADC
PAD
MAIN AMP
CRO
TYPE WRITER

Fig. 14.

In our case, $r_1 = r_2$ and so the relation between θ and ψ was always $\psi = \theta/2$. These adjustments were done to minimise the spread of the scattering angle due to the finite size of the scatterer.

The Ge-detector system (crystal specifications : 100 - mm^2 active area, 7-mm thickness, 3.5-mm distance from detector to crystal window face) used in our measurements has a resolution of the order of 176 eV (Full width at half maximum, FWHM) at a photon energy of 5.89 keV. With this and the ^{241}Am source, a very accurate determination of the number of elastically scattered photons was possible as these were well separated in the scattered spectrum from the component of inelastically scattered photons.

B. Method

At a large scattering angle θ, the expression for the differential elastic scattering cross section is given by

$$\frac{d\sigma^{el}}{d\Omega} = \frac{4\pi N_s \sin\theta \, r_1^2 \, r_2^2}{N_{at} \, I_o \, \epsilon \, A_d} \, G(\theta)$$

where N_s is the number of scattered photons per second, N_{at} is the number of atoms in the target, I_o is the number of monoenergetic photons that the source emits per second, ϵ is the efficiency and A_d the area of the detector and $G(\theta)$ is a geometrical correction

factor for absorption of incident and scattered photons in the target scatterer. The detector may be placed so as to receive the photon beam either reflected at or transmitted through the plane scatterer. $G(\theta)$ for the two cases are calculated from the expressions obtained by Kahane et al[48].

$$G(\theta) = \frac{e^{-\frac{\mu t}{\sin(\psi-\theta)}}\left[1 - e^{-\mu t\left(\frac{1}{\sin\psi} - \frac{1}{\sin(\theta-\psi)}\right)}\right]}{\mu t\left[\frac{1}{\sin\psi} - \frac{1}{\sin(\theta-\psi)}\right]}$$

for transmission geometry

$$G(\theta) = \frac{1 - e^{-\mu t\left[\frac{1}{\sin\psi} - \frac{1}{\sin(\theta-\psi)}\right]}}{\mu t\left[\frac{1}{\sin\psi} - \frac{1}{\sin(\theta-\psi)}\right]}$$

for reflection geometry

An auxilary experiment was carried out to determine the direct photon beam counts N_{Ge} by keeping the intrinsic Ge-detector at a large distance R from the source. N_{Ge} is related to the source strength I_o and the detector parameters through

$$N_{Ge} = \frac{I_o}{4\pi R^2} \epsilon A_d$$

The product $I_o A_d$ in the expression for cross section was thus eliminating by obtaining

$$\frac{d\sigma^{el}}{d\Omega} = \frac{4\pi\, N_s\, \sin\theta\, r_1^2\, r_2^2}{N_{at}\, 4\pi R^2\, N_{Ge}}\, G(\theta)$$

$$= \left(\frac{N_s}{N_{Ge}}\right)\left(\frac{r_1 r_2}{R}\right)^2\left(\frac{\sin\theta}{N_{at}}\right) G(\theta)$$

C. Measurements :

Differential elastic scattering cross sections at the angles 60° - 165° for target atoms Mo, Cd, Sn, Er, Yb and Ta were measured by using an ND 1100 multichannel analyser system coupled to a Ge-detector head at a conversion gain of 1024 with 512 channels and a spectrum storage time in the range 1-100 KS. The target foils used had the following dimensions

Target atom	Area (cm^2)	Thickness (cm)
Mo	25	0.01
Cd	25	0.005
Sn	19.63	0.01
Er	25	0.01
Yb	25	0.01
Ta	19.63	0.001

The angle of scattering (θ) and the angle (ψ) were measured very carefully and accurately each time by a telescopic arrangement. Each setting was checked to adjust the source, the

scatterer and the detector in the same horizontal plane. Background reading (without the scatterer at the scatterer holder) was always taken before and after each measurement. The average background result was subtracted from the reading obtained with the scatterer at the position of the scatterer holder. The position of the particular channels in the MCA in which the coherent component peak appeared was tested before and after the experiment to check for any channel shift. Total number of counts produced by coherently scattered γ-rays were obtained as the sum of channel contents after the subtraction of the background as usual. The number of channels was carefully chosen to include the whole photo peak area.

D. Experimental results:

The results from the set of elastic scattering measurements using 59.54 keV photons are presented in Table 21 together with experimental errors. The error arising from the superposition of coherent and incoherent peaks in the scattered spectra was completely eliminated, as is evident from an spection of Kg. The systemati errors include uncertainties in the determination of the photo peak area and uncertainties due to a variation in the detector background in the presence and absence of sample materials. Sources of random errors include statistical uncertainty in counting and uncertainties in measuring sample sizes, angles and distances. All these have been taken into consideration in the evaluation of measured

differential cross sections. Systematics errors have either been excluded effectively or accounted for the appropriate corrections. Owing to the finite size of the scatterer the error arising in measuring a certain scattering angle was negligible (e.g. $\Delta\Theta = \pm 0.25$ for $\Theta = 135^{\circ}$) since the angular width of the incident photon beam on the target of finite size was very small (8°). The corresponding error in $\frac{d\sigma}{d\Omega}$ was $\pm$ 0.004 b Sr^{-1} which was also negligible. The errors came in the range of about 4-9%.

Table 21. Measured differential cross sections for elastic scattering in barns per atom per steradian

Element Z	Scattering angle (deg)	Momentum transfer q (mc)	Measured cross section b/atom/Sr
^{42}Mo	60		1.406(±0.058)
	90		0.578(±0.027)
	135		0.335(±0.016
	165		0.427(±0.030)
^{48}Cd	90		0.997(±0.053)
	135		0.810(±0.040)
	165		0.656(±0.057)
^{50}Sn	60		1.780(±0.076)
	90		0.826(±0.040)
	135		0.687(±0.033)
^{68}Er	60		3.008(±0.116)
	135		0.824)(±0.032)
	150		0.937(±0.044)
	165		0.967(±0.074)